Predicting Human Thermal Comfort in a Transient Nonuniform Thermal Environment

John P. Rugh[1]✉, Robert B. Farrington[1], Desikan Bharathan[1], Andreas Vlahinos[2], Richard Burke[3], Charlie Huizenga[4], and Hui Zhang[4]

[1]National Renewable Energy Laboratory, 1617 Cole Blvd., Golden, CO 84010, U.S.A.

[2]Advanced Engineering Solutions, 4547 N. Lariat Drive, Castle Rock, CO 80104, U.S.A.

[3]Measurement Technology Northwest, 4211 24th Ave. West, Seattle, WA 98199, U.S.A.

[4]University of California, Berkeley, Center for Environmental Design Research, Berkeley, CA 94720, U.S.A.

email: john_rugh@nrel.gov

Abstract

The National Renewable Energy Laboratory (NREL) has developed a suite of thermal comfort tools to assist in the development of smaller and more efficient climate control systems in automobiles. These tools, which include a 126-segment sweating manikin, a finite element physiological model of the human body, and a psychological model based on human subject testing, are designed to predict human thermal comfort in transient nonuniform thermal environments such as automobiles. The manikin measures the heat loss from the human body in the vehicle environment and sends the heat flux from each segment to the physiological model. The physiological model predicts the body's response to the environment, determines 126 segment skin temperatures, sweat rates, and breathing rate, and transmits the data to the manikin. The psychological model uses temperature data from the physiological model to predict the local and global thermal comfort as a function of local skin and core temperatures and their rates of change.

Key Words

Thermal comfort, thermal manikin, human physiology, numerical modeling, automotive

1.0 Introduction

About 26 billion liters of fuel (equivalent to about 9.5% of our imported crude oil) are used annually to cool vehicle passenger compartments in the United States [Rugh and Hovland 2003]. Europe would use about 6.9 billion liters if all its vehicles were equipped with air conditioners. Japan uses about 1.7 billion liters to air condition its vehicles. These numbers can be reduced significantly with advanced climate control systems that reduce the solar load, efficiently and intelligently deliver conditioned air, and use more efficient equipment. However, there is a continuing need for sophisticated tools to evaluate the effectiveness of advanced climate control systems.

The objective of this project is to develop computational and physical models of human thermal physiology and thermal comfort to evaluate vehicle climate control systems. Specifically, NREL is developing a numerical model of human thermal physiology and psychology, and a thermal manikin that can be placed in vehicles. All will respond to the transient and extremely nonuniform thermal environments inside vehicle cabins. Industry can then use these tools to develop climate control systems that achieve optimal occupant thermal comfort with minimum power consumption [McGuffin et al. 2002].

2.0 Human Thermal Physiological Numerical Model

2.1 Description

The NREL Human Thermal Physiological Model, a three-dimensional transient finite element model, contains a detailed simulation of human internal thermal physiological systems and thermoregulatory responses. The model consists of two kinds of interactive systems: a human tissue system and a thermoregulatory system. The thermoregulatory system controls physiological responses, such as vasomotor control, sweating, and shivering. The human tissue system represents the human body, including the physiological and thermal properties of the tissues. The model was developed using the commercially available finite element software ANSYS. This software can compute heat flow by conduction, convection, and mass transport of the fluid, which makes it practical for simulating human heat transfer.

Human thermal response to an environment consists of convection within the circulatory and respiratory systems, and conduction within the tissues. The arms and legs consist of bone, muscle, fat, and skin. There are additional lung, abdominal, and brain tissues in the torso

and head segments. The model calculates the conduction heat transfer based on the temperature gradients between the tissue nodes.

Circulation heat transfer is modeled using a right-angled network of pipe elements within each body segment. The diameter of the pipes decreases from the center of each segment outward toward the skin and extremities. The flow in the pipes is modeled as Poiseuille flow and a convection coefficient is solved at each node in the pipe network. The diameters of the pipes in the skin layer can constrict or dilate depending on temperature distribution. The equations that control vasoconstriction/dilation are based on medical experiments [Smith 1991].

The human thermoregulatory system is modeled using vasoconstriction/dilation, sweating, shivering, and metabolic changes. The vasoconstriction/dilation response varies with skin and core temperatures, and with each body segment, because of the diameter of the pipes. The sweating response is a function of skin and core temperatures, and the number of sweat glands in each segment. The degree of shivering depends on skin and core temperatures, and the amount of muscle in each segment. The cardiac output or flow through the pipe network is a function of the metabolic rate and skin and core temperatures [Smith 1991].

2.2 Status

The physiological model was generated in sections using ANSYS. The sections consist of hand, lower arm, upper arm, foot, lower leg, and thigh, one each for the left and right sides. The body is developed as a torso together with neck and head. The limbs consist of bone, muscle, fat, and skin, each surrounding the previous layer. Special tissues for abdomen, lung, and brain are introduced in the torso and head volumes. Each part is generated individually and is populated with arteries and veins. The primary blood vessels join via capillaries placed adjacent to the skin layer. The blood vessel diameters are sized to allow blood to flow to each body part at an overall nominal pressure difference of 70 mmHg between the blood supply and return. The tissues are modeled using ANSYS Solid70 elements and the blood flow pipes use Fluid116 elements. Tissue properties are taken from tables provided by Gordon et al. [1976]. The overall masses and mass distribution for each part in the model compare favorably to those of a human. Deviations are nominally less than 5%.

An additional pipe network to simulate airflow through the trachea and lungs is also included in the torso. Each body part is connected to its adjacent part with veins and arteries. In the limbs, the tissues are not connected between parts. In the torso, which is modeled as an integral part, all tissues are connected.

The overall model consists of approximately 25,000 nodes and 25,000 elements. Because the model is very detailed, we can see a fairly complete picture of temperature distribution. An example for the hand is shown in Figure 1. For this simulation, blood flows into the supply arteries at 1380 cc/hr at 37?C. The hand's muscle and skin tissues generate heat at 750 W/m^3 and 1005 W/m^3, respectively. The hand is exposed to a lower temperature environment that is applied as a heat loss of 100 W/m^2 on its exposed surfaces. The resulting temperature distribution on the external surfaces is shown in Figure 1. The tip of the pinky attains the lowest temperature; the palm remains warm.

Figure 2 shows the temperature distribution over the body as well as a cross sectional view of the torso. The abdomen is warmer because of internal heat generation and relative isolation from the environment. The lung area remains cool because of breath flow. The brain mass reaches a moderate temperature between the two.

2.3 Technical Challenges

Given a set of heat flux boundary conditions on the skin, the model requires about 2 min to arrive at the steady-state temperature distribution. We expect to cut this time in half by streamlining the model and eliminating the large amount of input/output that occurs during a normal ANSYS run.

Future work will include modifying the model to run as a transient over a given amount of time and integrating with the data stream from the manikin. We have simulated this operation with one segment of the manikin and a corresponding model in ANSYS. We plan to extend that operation to the entire manikin.

The model can also be operated independently of the manikin to verify its behavior against published data. However, the model is currently configured to interact with the environment using only a heat flux boundary condition. To run as a stand-alone model, the interaction should occur via radiation, convection, and conduction. Convection should also include sensible and latent heat transfer. To accommodate all these modes of heat transfer, the model requires additional surface shell elements. Additional work is needed to implement these elements in the model. Our capabilities are therefore

limited in comparing model predicted data with experimental results at this time.

3.0 Human Thermal Physical Model – The ADvanced Automotive Manikin (ADAM)

3.1 Description

The manikin acts as a heat transfer sensor that mimics a real three-dimensional body. It senses the difficult-to-model local sweat evaporation, convection, and radiation processes that are highly dependent on local microclimate. The manikin can also be clothed to accurately depict the sweat transport of a clothed human and analyze other clothing effects. The manikin is primarily designed as an integrated tool for use with the Human Thermal Physiological Model and Human Thermal Comfort Model, but it can also operate as a stand-alone device to test clothing or environments following traditional control schemes.

The manikin is designed with the following general capabilities and characteristics:

- Detailed spatial and rapid temporal control of surface heat output and sweating rate.
- Surface temperature response time approximating human skin.
- Human-like geometry and weight with prosthetic joints to simulate the human range of motion.
- Breathing with inflow of ambient air and outflow of warm humid air at realistic human respiration rates.
- Complete self-containment, including battery power, wireless data transfer, and internal sweat reservoir for at least 2 hr of use with no external connections.
- Rugged, durable, low-maintenance construction.

The geometry of the manikin was designed to match the 50^{th} percentile American male. The manikin is approximately 1.75 m tall. A NURBS digital model of the human body was reshaped in CAD to comply with the 50^{th} percentile target and allow the manikin to be digitally manufactured.

The manikin's fundamental components are the 126 individual surface segments, each with a typical surface area of 120 cm^2. Each segment is a stand-alone device with integrated heating, temperature sensing, sweat distribution and dispensing, and a local controller to manage the closed loop operation of the zone. The sweating surface is all-metal construction optimized for thermal uniformity and response speed. Variable porosity within the surface provides lateral sweat distribution and flow regulation across the zone. Distributed resistance wire provides uniform heating, and is backed up by an insulative layer that improves structural rigidity. The single zone controller, including flow control valving, is mounted directly behind the zone [Burke et al. 2003].

The manikin's skeleton is composed of laminated carbon fiber, which supports its structure, houses all internal components, and provides mounting locations for surface segments. The joints connect the skeleton parts to give the manikin a human-like form. The adjustable friction joints are pre-tensioned so it can be posed in specific human positions. The wiring harness and sweat tubes pass through the joints.

In a vehicle, the manikin can operate with no external cabling; rather, it uses an internal battery power source (four internal NiMH battery modules in the torso and thighs) and a wireless communication system. For wireless communication, data are transferred via 900 MHz spread spectrum transceivers. For applications that do not require wireless operation, the system can be plugged into an external power supply and communication port for continuous operation and battery charging.

3.2 Status

All segments are complete, although sensor, heater, and fluid problems have delayed the full operation of 11 segments. The manikin has been assembled (Figure 3), and full testing has been initiated. The breathing system has not yet been incorporated. More details are available in Burke et al. [2003].

3.3 Technical Challenges

In very dry conditions, evaporation rates may be so high that the segment surface is not completely wetted by the sweat. If the locations where the temperatures are measured are not wetted, an incorrect temperature reading may result. The segment emissivity is lower than skin emissivity, which increases the heat loss to the environment. The response time of the manikin to a transient environment and to a change in the set point temperatures will be carefully assessed. When the manikin is seated, certain segments will recess into its interior. The Human Thermal Physiological Model will need to recognize this condition and adjust appropriately. More details are available in Burke et al. [2003].

4.0 Human Thermal Comfort Empirical Model

4.1 Description

We performed 109 human subject tests under a range of steady-state and transient thermal conditions to explore

the relationship between local thermal conditions and perception of local and overall thermal comfort. The tests include collection of core and local skin temperatures as well as subjective thermal perception data obtained via a simple form. These data are used to develop a predictive model of thermal comfort perception [Zhang et al. 2003].

The human subject testing was conducted in the Controlled Environmental Chamber at the University of California-Berkeley. The subject first stayed in a temperature-controlled water bath for 15 min to decrease the time needed for the body to reach a stable, repeatable initial condition. After drying, the subject was fitted with a harness of skin surface temperature sensors under a thin leotard. In each test, an air sleeve was connected to an individual segment of the leotard and supplied controlled temperature air to provide local heating and cooling. The subject voted his or her overall and local thermal sensation and comfort approximately every minute (see Figure 4). After 10–20 minutes, the local heating or cooling was removed. The procedure was repeated for other segments.

The skin temperature measurement harness had 28 fine gauge thermocouples to measure the skin temperatures at standardized locations on the body. The thermocouples were soldered onto an 8 mm copper disk and taped to the skin to allow very fast response during temperature transients.

A wireless sensor was used to measure core temperature. The subject swallowed the sensor before the test. As the sensor passed through the digestive tract, it provided a high-resolution measurement of the core temperature.

We used the 9-point thermal sensation scale, extending the ASHRAE scale with "very cold" and "very hot." We used an independent comfort scale rather than the combined Bedford scale since the highly asymmetric and transient conditions produced during the test meant that a cold or hot sensation could be quite comfortable.

4.2 Status

The subject testing and analysis are complete. Details are available in Zhang et al. [2003].

4.3 Technical Challenges

The test subject sample size was somewhat limited, and did not include a wide variety of ages, weights, and body compositions. Since the potential number of test permutations is very large, a subset of tests was carefully selected. Correlating global thermal comfort proved to be a complicated process. Details are available in Zhang et al. [2003].

5.0 Thermal Comfort Model Integration

5.1 Description

Each tool discussed in this paper addresses an element of the total human comfort perception. The integrated thermal comfort prediction system consists of the thermal manikin, Human Thermal Physiological Model, and the Human Thermal Comfort Model. The manikin represents the physical hardware components in this comfort toolbox. It provides a true body positioned in a vehicle to measure the transient thermal response with extremely high spatial density. The finite element model provides the manikin with a control algorithm that closely mimicks human response. The real-time psychological comfort model uses this response to output the end goal of the system—human perceptions of local and global thermal comfort versus time.

The manikin is essentially a surface sensor that measures the rate of heat loss at each surface segment. The skin heat transfer rates are sent to the physiological model, which computes the skin and internal temperature distribution and surface sweat rates. This information is then sent back to the manikin, which generates prescribed the skin temperatures and surface sweat rates, and breathing rate. This loop continues to provide a transient measurement tool. Within each period of the loop, the temperature distribution and rate of temperature change is sent to the psychological thermal comfort model. The temperature distribution and rates of change are then converted to perceptions of local and global sensation and comfort, which are displayed graphically versus time on a laptop computer.

5.2 Status

All components of the thermal comfort model and initial interface testing are complete.

5.3 Technical Challenges

Since the manikin and models have different time constants, the control software will need to be optimized to minimize run time and maximize time step. Measuring low heat fluxes at low temperature differences is difficult, and may cause control stability issues. Validating the entire process will be a challenge.

6.0 Conclusions

We have developed the three major systems necessary for predicting thermal comfort in a transient, nonuniform thermal environment: a physiological model of the human thermal regulatory system, a physical model (manikin) of the human body including heating and sweating, and an empirical model to predict local and global thermal sensation and comfort. Initial integration of the three components has been completed and is being validated. Each component (as well as the interaction of the models) has presented its own challenges. We plan to use the integrated models in vehicle applications to develop and evaluate fuel-saving climate control systems.

7.0 References

Burke, R.; Rugh, J.; and Farrington R. (2003) ADAM – the Advanced Automotive Manikin, 5th International Meeting on Thermal Manikins and Modeling, Strasbourg, France.

Gordon, R. G.; Roemer, R. B.; and Horvath, S. M. (1976) A Mathematical Model of the Human Temperature Regulatory System – Transient Cold Exposure Response. IEEE Transactions on Biomedical Engineering 23, no. 6: 434-444.

McGuffin, R.; Burke, R.; Zhang, H.; Huizenga, C.; Vlahinos, A.; and Fu, G. (2002) "Human Thermal Comfort Model and Manikin," SAE paper #2002-01-1955, 2002 SAE Future Car Congress, Arlington, VA, June 4, 2002.

Rugh, J. and Hovland, V. (2003) National and World Fuel Savings and CO_2 Emission Reductions by Increasing Vehicle Air Conditioning COP. Proceedings from the 2003 Alternate Refrigerant Systems Symposium in Phoenix, AZ.

Smith, C. E. (1991) A Transient, Three-Dimensional Model of the Human Thermal System. PhD Thesis, Kansas State University.

Zhang, H.; Huizenga, C.; and Arens E. (2003) Thermal Sensation and Comfort in a Transient Non-Uniform Thermal Environment, 5th International Meeting on Thermal Manikins and Modeling, Strasbourg, France.

Acknowledgments

This work was supported by DOE's Office of FreedomCAR and Vehicle Technologies (OFCVT). The authors appreciate the support of DOE Program Managers Robert Kost and Roland Gravel; Terry Penney, NREL's OFCVT Technology Manager; and Barbara Goodman, Director of the Center for Transportation Technologies and Systems.

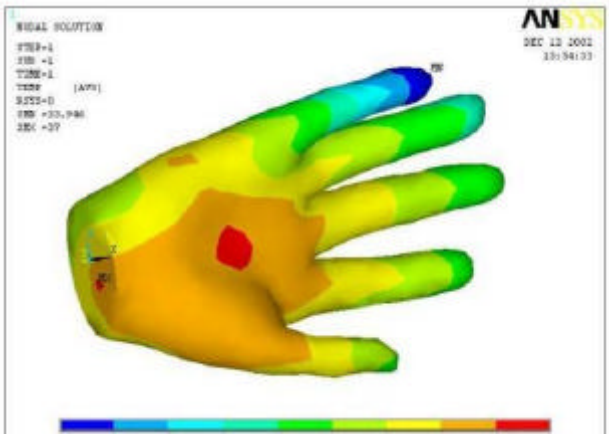

Figure 1. Hand Temperature Distribution

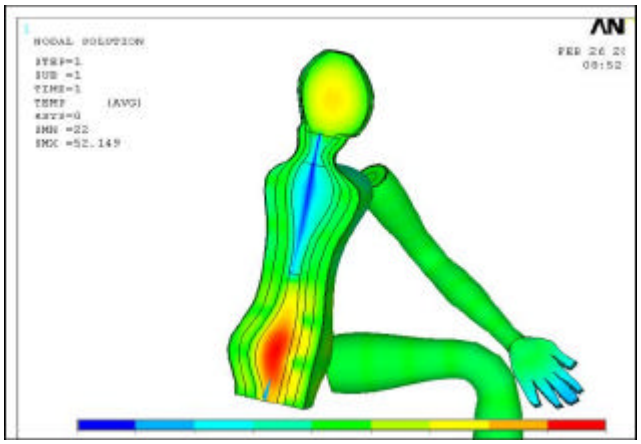

Figure 2. Temperature Distribution through Body Core

Figure 3. ADAM

Figure 4. Thermal Sensation and Comfort Testing